Geometric Phase Associated with Mode Transformations of Optical Beams Bearing Orbital Angular Momentum

E. J. Galvez, P. R. Crawford, H. I. Sztul, M. J. Pysher, P. J. Haglin, and R. E. Williams
Department of Physics and Astronomy, Colgate University, Hamilton, New York 13346, USA
(Received 24 October 2002; revised manuscript received 21 January 2003; published 20 May 2003)

We present direct measurements of a new geometric phase acquired by optical beams carrying orbital angular momentum. This phase arises when the transverse mode of a beam is transformed following a closed path in the space of modes. The measurements were done via the interference of two copropagating optical beams that pass through the same interferometer parts but acquire different geometric phases. The method is insensitive to dynamical phases. The magnitude and sign of the measured phases are in excellent agreement with theoretical predictions.

DOI: 10.1103/PhysRevLett.90.203901 PACS numbers: 42.25.Hz, 03.65.Vf

Optical beams bearing orbital angular momentum (OAM) have been recently recognized as potential systems for doing N-bit quantum computation [1–3]. This is possible because these light beams can encode a large number of OAM states in the phase structure of the beam. This is in contrast to polarization states of light, which are inherently binary (e.g., right and left circular polarization). Quantum computation with OAM-bearing beams will require the generation, transformation, and detection of OAM states [4]. Furthermore, a geometric phase, or Berry's phase [5], has been identified as a potential means of doing quantum computation [6,7]. A geometric phase acquired by an optical beam depends on the geometry of the path followed by the beam. This path may be in configuration space (spin redirection phase) [8], polarization state space (Pancharatnam phase) [9] or, as shown here, in mode space. Because of its dependence on a sequence of transformations and not on the optical path length, geometric phase is a much more robust phase, insensitive to vibrations and other mechanical effects [6].

In 1992, a study of the OAM of Gaussian beams in high-order modes brought forth a method to perform transformations between two families of modes [10]. Laguerre-Gauss (LG) and Hermite-Gauss (HG) modes follow from solutions to the paraxial equation in cylindrical and rectangular coordinates, respectively [11]. Modes LG_p^ℓ with radial index p and azimuthal index ℓ carry an OAM of $\ell\hbar$ per photon. Modes HG_{nm} (TEM_{nm}) do not carry OAM. The order of these modes is given by $N = 2p + |\ell| = n + m$ [12]. The mode transformers use astigmatic lenses to insert unequal Gouy phases to transformer's eigenstates, similar to the way a wave plate introduces a phase between its polarization eigenstates. The possibility of a geometric phase arising from mode transformations was first proposed by van Enk [13]. More recently, evidence of a geometric phase in mm waves with nonideal mode transformers has been reported [14]. Direct measurements of the geometric phase in optical mode transformations have remained elusive until now because these measurements rely on the interference of the mode-transforming beam with a reference beam. Dynamical phases produced by rotating astigmatic mode transformers make the interferograms critically sensitive to the alignment of these components. In this article we present the first direct measurements of this geometric phase using a new technique described below.

Mode transformations can be understood analytically using matrix algebra [15,16]. For example, a minimal sequence of three transformations T that take the input mode ψ through two intermediate steps and back to its initial state can be represented by

$$T\psi = e^{i\phi}\psi, \tag{1}$$

where the total transformation can be decomposed into a product of transformations $T = T_3T_2T_1$. In general, the phase of the final state differs from that of the initial state by $\phi = \phi_d + \phi_g$, where ϕ_d and ϕ_g are the dynamical and geometric phases, respectively. If only the topology of the path is altered, then only ϕ_g varies.

One of the advantages of geometric phase is that in many cases it can be analyzed purely geometrically, which adds simplicity to the problem. The "orbital" Poincaré sphere has been proposed as the geometrical construction to represent the space of first-order modes [17], and its structure has been shown to possess SU(2) symmetry [18]. In analogy to the space of states of polarization, points in the eastward direction along the equator of the sphere (Fig. 1) correspond to HG modes of orientations that rotate clockwise [19]. The North and South poles of the sphere correspond to the LG_0^{+1} and LG_0^{-1} modes, respectively. Points of equal phase in a LG_0^{+1} (LG_0^{-1}) beam form a right-handed (left-handed) corkscrew spiral along the direction of propagation. Equivalently, the phase of the wave on a transverse plane advances counterclockwise (clockwise).

Mode transformations involving a change in latitude on the sphere are obtained using astigmatic mode converters [10]. A "ϕ-converter" introduces a phase ϕ between the

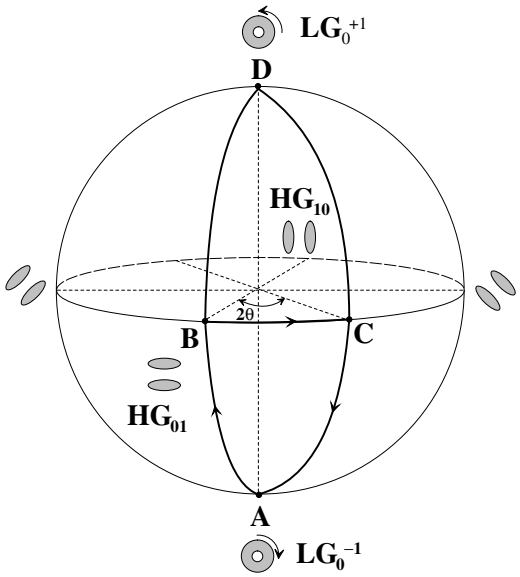

FIG. 1. Orbital Poincaré sphere for first order modes.

HG-mode eigenstates of the converter, which are antipodes on the sphere. Via the SU(2)-SO(3) homomorphism, unitary mode transformations correspond to rotations on the orbital Poincaré sphere. If we represent the HG_{10} and HG_{01} modes as the eigenstates, $|HG_{10}\rangle = (1\ 0)^T$ and $|HG_{01}\rangle = (0\ 1)^T$, then the ϕ-conversion matrix given by [16]

$$C(\phi) = \begin{pmatrix} e^{-i\phi/2} & 0 \\ 0 & e^{i\phi/2} \end{pmatrix} \tag{2}$$

corresponds in the Poincaré sphere to a left-handed rotation by ϕ about the eigenvector of the transformation with eigenvalue $\exp(i\phi/2)$, which in this case is HG_{01}. Experimentally, the device that exerts this type of conversion uses a pair of cylindrical lenses with their focal lines parallel. We will hereafter refer to this direction as the principal axis of the converter ("PA" in Fig. 2). This axis is also the phase inversion symmetry axis of the HG mode that is an eigenvector of the converter. For the case of the HG_{01} mode this corresponds to the horizontal axis. We describe converters in other orientations by rotations of the matrix given by Eq. (2),

$$C(\phi, \alpha) = R(-\alpha)C(\phi)R(\alpha), \tag{3}$$

where $R(\alpha)$ is a 2×2 unitary rotation matrix [15,16]. Thus, an $\alpha > 0$ rotation moves the converter eigenvector westward on the sphere. In the laboratory this corresponds to rotating the principal axis of the converter counterclockwise by the same amount.

Consider the set of transformations involved in the path *ABCA* of Fig. 1. We break the path into three sections: *AB*, *BC*, and *CA*. The paths *AB* and *CA* are $\pi/2$ transformations produced by well known $\pi/2$-converters [12]. The matrix for the conversion in path *AB* is $T_{AB} = C(\pi/2, -\pi/4)$. It converts the LG_0^{-1} mode [$|LG_0^{-1}\rangle = 2^{-1/2}(1\ i)^T$] into the HG_{01} mode, involving an exchange of OAM of $\hbar$ between the light and the optical system. The converter providing this transformation has its principal axis rotated clockwise 45° from the horizontal (see Fig. 2), with eigenvector $2^{-1/2}(1\ 1)^T$ [20]. Path *BC* is a rotation by θ, described by $T_{BC} = R(\theta)$. The return path *CA* corresponds to the $\pi/2$ conversion described by $T_{CA} = C(\pi/2, \pi/4 - \theta)$. This returns the mode of the beam to the LG_0^{-1} mode, and restores OAM to the beam. Since these transformations involve geodesics on the Poincaré sphere they do not introduce any dynamical phases [21]. Therefore, we can set $\phi_d = 0$ for simplicity. After algebraically simplifying the total transformation matrix $T_{ABCA} = T_{CA}T_{BC}T_{AB}$, we find that it is a rotation matrix. This is a simple and elegant result that arises only for initial states that are pure OAM eigenstates. As expected, diagonalizing it gives eigenvalues $\exp(-i\theta)$ and $\exp(i\theta)$ and eigenvectors LG_0^{+1} and LG_0^{-1}, respectively [16]. Thus, from Eq. (1) with $T = T_{ABCA}$ and $\psi = |LG_0^{-1}\rangle$ we get that the geometric phase is $\phi_g = \theta$ [22]. In analogy to Pancharatnam phase, the geometric phase is given by $\phi_g = -\Omega/2$, where Ω is the solid angle enclosed by the path [17]. Thus for the path *ABCA* of Fig. 1 the geometrical picture also predicts $\phi_g = \theta$.

The procedure in these experiments was to introduce a geometric phase on a LG_0^{-1} beam, change it, and measure it via interference with a reference LG_0^0 (TEM_{00}) beam. However, it is very difficult to perform this experiment if the two interfering beams travel different physical paths. As described below, one of the $\pi/2$ converters has a pair of cylindrical lenses that must rotate. Slight

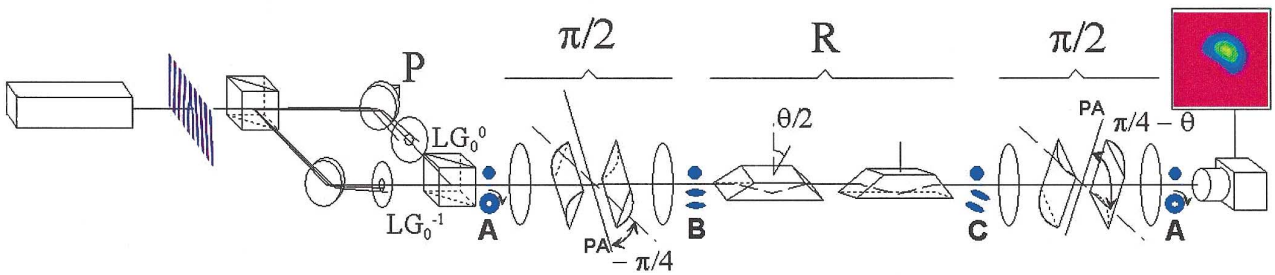

FIG. 2 (color). Schematic diagram of the experimental setup for inserting a variable geometric phase via the mode transformations associated to the path *ABCA* in Fig. 1.

misalignments in the positions of the center of the cylindrical lenses with respect to their rotation axes result in a deflection of the beam, introducing dynamical phases that overwhelm the geometric phases involved. Our solution to this problem was to send the reference beam through the mode transformers collinearly with the LG_0^{-1} beam. Since the LG_0^0 mode is the only one in its mode space it does not get modified by a sequence of mode transformers [12]. Any dynamical phases present are introduced to both beams and are therefore effectively canceled out.

A simplified diagram of our experimental setup is shown in Fig. 2. It consisted of a light source, a Mach-Zehnder interferometer, a sequence of mode transformers, and a beam imaging system. The light source was a Gaussian beam from a 5-mW HeNe laser in a LG_0^0 mode with vertical linear polarization. It was sent to a charge-1 forked binary diffraction grating, which was computer generated, printed, and photoreduced [23]. We oriented the grating with its fork "handle" pointing up, as shown in Fig. 2. In the top path of the interferometer shown in the figure we used an iris to allow only the zero order (i.e., in the LG_0^0 mode) to go through. The mirror in this arm was mounted on a piezo stack (labeled "P" in Fig. 2) to change the interference by deliberately adding a dynamical phase to one of the beams. In the lower arm of the interferometer an iris blocked all diffraction orders except for the first order on the left-hand side of the zero order, which was in the LG_0^{-1} mode. The interferometer had nonpolarizing cube beam splitters, with the second one positioned to make the two beams collinear. A telescope located after the Mach-Zehnder interferometer (not shown) adjusted the radius of curvature of the phase front to simplify mode matching.

Each of the two $\pi/2$-converters consisted of a pair of parallel cylindrical lenses of focal length $f = 50$ mm separated by a distance $d = \sqrt{2}f$. These lenses were between a pair of spherical lenses ($f = 470$ mm) to provide the mode matching condition [12]. The second converter had its cylindrical lenses mounted on a rotation stage that allowed its axis and the position and axial orientation of the cylindrical lenses to be independently adjusted. The rotator was a pure image rotator made of two Dove prisms in series. When the transverse symmetry axis of the first (second) Dove prism was turned an angle $\theta/2$ ($-\theta/2$) the incident image was rotated by θ. The beam profile of the output beam was recorded with a charge-coupled device (CCD) camera connected to digitizing hardware and software.

Figure 3(a) shows a profile of the LG_0^{-1} mode after experiencing the two differential wave front rephasings that the path *ABCA* entails. It displays the "doughnut" profile that is characteristic of OAM eigenstates. The profile of the LG_0^0 beam after going through the system is shown in Fig. 3(b). The profile of each beam was taken after blocking the other beam in the Mach-Zehnder interferometer. When both beams were unblocked they

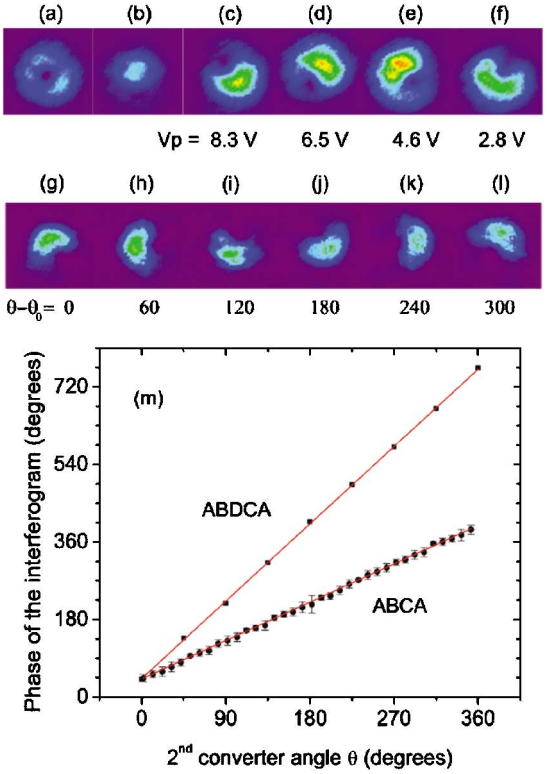

FIG. 3 (color). False color images of (a) LG_0^{-1} mode, (b) LG_0^0 mode, and the interference between them: (c)–(f) after introducing a dynamical phase to the LG_0^0 beam and (g)–(l) in a different experiment, when the LG_0^{-1} mode acquired a geometric phase θ. (m) A graph of the phase extracted from a set of the interferograms for paths *ABCA* (circles) and *ABDCA* (squares) as a function θ and linear fits to the data (lines).

formed an interference pattern that consisted of a broad peak on the rim of the doughnut at the azimuth angle where the two beams were in phase. At the opposite end of the doughnut the beams were out of phase, so the overall pattern had an oval shape with an off-center maximum. A simulation of this pattern is shown in the inset of Fig. 2. We could verify the phase dependence of the pattern of Fig. 3(a) by introducing a dynamical phase between the two beams. This was done by varying the voltage on the piezo V_P. By decreasing V_P we increased the optical path length of the LG_0^0 beam relative to the LG_0^{-1} beam. This advanced the phase of the LG_0^{-1} mode relative to the LG_0^0 mode, making the interference maximum rotate clockwise after the second $\pi/2$ converter, but because there was a mirror (not shown) between the latter and the camera, the recorded maximum rotated counterclockwise. Figures 3(c)–3(f) show a sequence of patterns for different values of V_P ($d\phi_d/dV_P = 54(2)$ degrees/V). These are consistent with the expected phase structure of LG_0^{-1} and with the profile of Fig. 3(a).

As discussed earlier, if we rotate the first Dove prism by $\theta/2$ and the second $\pi/2$-converter by θ (with $V_P = 0$) such that the first-order mode of the beam follows the path *ABCA* in Fig. 1, this should introduce a geometric

phase $\phi_g = \theta$. Indeed, the data set of Figs. 3(g)–3(l) shows that as θ was increased the maximum in the interferograms as recorded by the camera moved counterclockwise, consistent with the phase of LG_0^{-1} increasing relative to that of LG_0^0. We took several data sets and found the accumulated phase to be consistent and robust. Figure 3(m) shows a complete data set (circles) taken for increments of θ of 10° over a 360° range. The relative phase between the two beams was obtained by measuring the azimuth angle of the maximum of the pattern. This angle was taken as a measure of the phase. As shown in the figure, the measured angles showed a linear dependence with θ. A least squares linear fit to the data gave $\phi_g = (0.99 \pm 0.01)\theta + (42 \pm 2)°$. The slope's magnitude and sign are in excellent agreement with the prediction.

We chose path *ABCA* to demonstrate the geometric phase via wave front rephasing in a path where the intermediate states were not LG eigenstates. A second measurement involved the path *ABDCA* of Fig. 1. Experimentally, we used the same method as before. After the Mach-Zehnder interferometer, a fixed π-converter consisting of a pair of parallel cylindrical lenses ($f = 50$ mm) separated by $d = 2f$ transformed the LG_0^{-1} mode into a LG_0^{+1} mode [$|LG_0^{+1}\rangle = 2^{-1/2}(1\ -i)^T$] following the path *ABD*, with $T_{ABD} = C(\pi, -\pi/4)$. This corresponded to an OAM exchange of $2\hbar$. Past the first π-converter, a second rotatable π-converter returned the mode to the initial state via the path *DCA*, with $T_{DCA} = C(\pi, \pi/4 - \theta)$, restoring the OAM to the beam. The predicted geometric phase for this closed path is $\phi_g = 2\theta$. This is consistent with a solid angle enclosed by the curve, which is twice that of the previous case. As before, a measurement of the orientation of the interference pattern as recorded by the camera gave a measure of the phase of the LG_0^{-1} beam relative to the LG_0^0 beam. A least squares linear fit to the data, shown in Fig. 3(m) (squares), gave $\phi_g = (2.00 \pm 0.01)\theta + (43 \pm 2)°$, in excellent agreement with the prediction. The error bars for these data were smaller than the symbols.

Since OAM eigenstates have a phase structure of the form $\exp(i\ell\varphi)$, with φ being the transverse angular coordinate, any phase-shifting transformation is a rotator. Using an image rotator such as a pair of Dove prisms would also introduce a geometric phase, but via spin redirection phase [8]. As the light passes through the Dove prisms, these change the direction of the light spin such that it describes a closed path in configuration space [24], thus resulting in a geometric phase. Previously measured frequency shifts resulting from the rotation of OAM-bearing microwave beams using Dove prisms are a result of such an evolving geometric phase [25].

In conclusion, we demonstrated that mode transformations of higher-order Gaussian beams bearing OAM lead to a new optical geometric phase. The experimental results are in excellent agreement with the theoretical description. We also showed that dynamical phases can be eliminated in the measurement of the geometric phase by sending the beam with the mode of interest together with the reference beam collinearly through the optical system. These experiments can also be performed with a reference beam in a mode other than the LG_0^0 mode, in which case the geometric phase of the reference beam will also need to be accounted [26]. This method is robust and may find applications in new forms of quantum computation. All of these geometric phases arose from transformations involving a change in the OAM of the modes. They support the conjecture that geometric phase arises from the exchange of angular momentum between the light and the optical system [13].

We thank V. Matos for the forked gratings and S. Malin and G. Nienhuis for useful discussions. This work was funded by a grant from Research Corporation and National Science Foundation Grant No. PHY-9988004.

[1] A. Mair *et al.*, Nature (London) **412**, 313 (2001).
[2] G. Molina-Terriza, J. P. Torres, and L. Torner, Phys. Rev. Lett. **88**, 013601 (2002).
[3] A. Vaziri, G. Weihs, and A. Zeilinger, Phys. Rev. Lett. **89**, 240401 (2002).
[4] J. Leach *et al.*, Phys. Rev. Lett. **88**, 257901 (2002).
[5] M. V. Berry, Proc. R. Soc. London A **392**, 45 (1984).
[6] J. A. Jones *et al.*, Nature (London) **403**, 869 (2000).
[7] L.-M. Duan, J. I. Cirac, and P. Zoller, Science **292**, 1695 (2001).
[8] R. Chiao and Y.-S. Wu, Phys. Rev. Lett. **57**, 933 (1986).
[9] R. Bhandari and J. Samuel, Phys. Rev. Lett. **60**, 1211 (1988).
[10] L. Allen *et al.*., Phys. Rev. A **45**, 8185 (1992).
[11] A. Siegman, in *Lasers* (University Science Books, Mill Valley, CA, 1986).
[12] M. W. Beijersberger *et al.*, Opt. Commun. **96**, 123 (1993).
[13] S. J. van Enk, Opt. Commun. **102**, 59 (1993).
[14] G. F. Brandt, Int. J. Infrared Millimeter Waves **21**, 505 (2000).
[15] L. Allen, J. Courtial, and M. J. Padgett, Phys. Rev. E **60**, 7497 (1999).
[16] A. T. Oneil and J. Courtial, Opt. Commun. **181**, 35 (2000).
[17] M. J. Padgett and J. Courtial, Opt. Lett. **24**, 430 (1999).
[18] G. S. Agarwal, J. Opt. Soc. Am. A **16**, 2914 (1999).
[19] All modes described here are referred to what one observes when the mode is projected on a screen.
[20] The angles of rotation of the direction of the eigenvectors on the sphere are twice those in the laboratory.
[21] R. Bhandari, Phys. Lett. A **138**, 469 (1989).
[22] For $\psi = |LG_0^{+1}\rangle$ the same transformation describes the path $DB'C'D$ on the sphere of Fig. 1, where B' and C' are the antipodes of B and C, respectively.
[23] N. R. Heckenberg *et al.*, Opt. Lett. **17**, 221 (1992).
[24] E. J. Galvez and C. D. Holmes, J. Opt. Soc. Am. A **16**, 1981 (1999).
[25] J. Courtial *et al.*, Phys. Rev. Lett. **80**, 3217 (1998).
[26] E. J. Galvez, H. I. Sztul, and P. J. Haglin (to be published).